HHS Public Access

Author manuscript

Org Biomol Chem. Author manuscript; available in PMC 2022 August 28.

Published in final edited form as:

Org Biomol Chem. 2021 August 05; 19(30): 6697–6706. doi:10.1039/d1ob00742d.

Discrimination of Enantiomers of Amides with Two Stereogenic Centers Enabled by Chiral Bisthiourea Derivatives Using ^{1}H NMR Spectroscopy

Hanchang Zhang[a], **Hongmei Zhao**[b], **Jie Wen**[a], **Zhanbin Zhang**[a], **Pericles Stavropoulos**[c], **Yanlin Li**[a], **Lin Ai**[a], **Jiaxin Zhang**[a]

[a]College of Chemistry, Beijing Normal University, Beijing 100875, P. R. China.

[b]State Key Laboratory of Information Photonics and Optical Communications, School of Science, Beijing University of Posts and Telecommunications, Beijing 100876, P. R. China

[c]Department of Chemistry, Missouri University of Science and Technology, Rolla, Missouri 65409, USA

Abstract

Enantiomers of a few new amides containing two stereogenic centers have been derived from *D*- and *L*-α-amino acids as guests for chiral recognition by ^{1}H NMR spectroscopy. A variety of chiral amides with two or more stereogenic centers often exist in products of catalytical asymmetric synthesis, natural products or its total synthetic products, and chiral drugs. It would be a challenging and meaningful work to explore the their chiral recognition. For this purpose, a class of novel chiral bisthiourea derivatives **1**–**9** has been synthesized from (1*S*, 2*S*)-(+)-1,2-diaminocyclohexane, *D*-α-amino acids, and isothiocyanates as chiral solvating agents (CSAs). CSAs **1**–**9** proved to afford better chiral discriminating results towards most amides with two stereogenic centers, which have been rarely studied as chiral substrates by ^{1}H NMR spectroscopy. Especially, CSAs **7**, **8** and **9**, featuring 3,5-bis(trifluoromethyl)benzene residues, exhibit outstanding chiral discriminating capabilities towards all amides, providing well-separated ^{1}H NMR signals and sufficiently large nonequivalent chemical shifts. To test their practical application in determination of enantiomeric excess, ^{1}H NMR spectra of chiral amides (G**16**) with different optical purities were measured in the presence of CSAs **7** and **8**, respectively. Their ee values (up to 90%) were accurately calculated by intergation of the *NH* proton of the CO*NH*Ph group of G**16**. To better understand the chiral discriminating behavior, Job plots of (±)-G**16** with CSA **7** and (±)-G**17** with CSA **8**, the association constants (K_a) of (*S,R*)-G**16** and (*R,S*)-G**16** with CSA **7** were evaluated, respectively. In order to further reveal any underlying intermolecular hydrogen bonding interactions, theoretical calculations of enantiomers of (*S,R*)-G**16** and (*R,S*)-

linai@bnu.edu.cn, zhangjiaxin@bnu.edu.cn.

Conflicts of interest

There are no conflicts to declare.

†Electronic Supplementary Information (ESI) available: Synthetic procedures of characterization of CSAs **1**–**9** and enantiomers of amides **16**–**27**, and their NMR and HRMS spectra, ^{1}H NMR spectra of chiral recognition of (±)-G**16**–**27** in the presence of CSAs **1**–**9** See DOI:10.1039/x0xx00000x

G**16** with CSA **7** were performed by means of the hybrid density functional theory (B3LYP) with the standard basis sets of 3–21G of the Gaussian 03 program, respectively.

Graphical Abstract

Enantiomers of amides with two stereogenic centers have been effectively discriminated in the presence of chiral bisthiourea derivatives as chiral solvating agents by ^{1}H NMR spectroscopy.

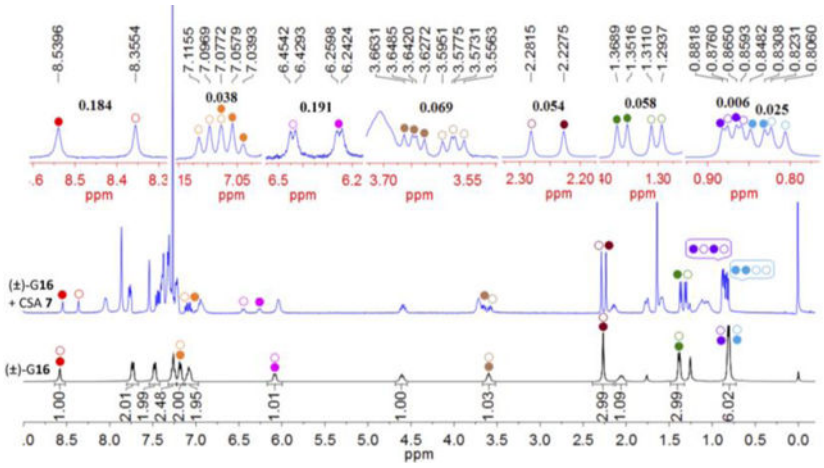

Introduction

The determination of enantiomeric excess (ee) of chiral compounds is among the most fundamental undertakings of chirality and related studies, in various fields such as in catalytic asymmetric chemistry, biology and pharmaceutical science.[1] For this purpose, various methods and techniques have been developed and utilized. Among them, high performance liquid chromatography (HPLC) is the most classic and traditional technique for separation of enantiomers and determination of enantiomeric excess.[2] In addition, other methods and techniques, such as NMR spectroscopy,[3] circular dichroism (CD),[4] mass spectrometry (MS),[5] X-ray crystallography,[6] UV/vis and fluorescence spectroscopy,[7] have also been developed to explore discrimination of enantiomers, separately or in tandem. Especially, ^{1}H NMR spectroscopy has been advanced more rapidly in the field of chiral recognition due to several apparent advantages, including fast and accurate application, convenient measurements, as well as employment of low amounts of hosts and guests.[8] Of course, excellent and efficient chiral auxiliaries play a key role in the study of chiral recognition by means of ^{1}H NMR spectroscopy. As a result, various chiral derivatizing agents (CDAs),[9] and chiral solvating agents (CSAs), including chiral bisurea and bisthiourea derivarives,[10] have been synthesized and evaluated for establishing highly effective chiral auxiliaries. Herein, a class of novel chiral bisthiourea derivatives has been synthesized as chiral solvating agents for chiral recognition, engaging various kinds of readily interchangeable, *D*-α-amino acids (phenylglycine, phenylalanine and valine), (1*S*,2*S*)-(+)-1,2-diaminocyclohexane, and phenylisothiocyanate (or its respective derivatives).

In the field of chiral recognition, chiral substrates with only one stereogenic center, such as chiral amines,[11] amino alcohols,[12] alcohols,[13] carboxylic acids,[14] carbonyl compounds,[15] amino acids and their derivatives,[16] have been often used as guests in the presence of chiral auxiliaries for ee determination by ^{1}H NMR spectroscopy. In contrast, chiral recognition of chiral substrates with two or more stereogenic centers has been rarely reported.[17] However, such chiral substrates often exist in products of catalytic asymmetric synthesis, and also participate in the total synthesis of natural products and preparation of chiral drugs.[18] Importantly, different enantiomers may have different biological and pharmacological activities, and even result in the opposite physiological effects.[19] Thus, analysis of optical purity and differentiation of enantiomers of these chiral analytes, are highly important undertakings, to be used therapeutically in the context of the clinical chiral drugs. Among them, the amide group is one of the most essential and important moieties[20] and also the basic building block in proteins, associated with the formation of peptide bonds.[21] For example, an analysis of chemical reactions used in current medicinal chemistry (2014) revealed that the most frequently used chemical reactions were amide bond formation methodologies, accounting for 16% of all reactions. [22] In this paper, enantiomers of several chiral amides with two stereogenic centers (*SR* and *RS*) were prepared by using *D*- and *L*-α-amino acids as chiral sources, and their chiral recognition was studied in the presence of chiral bisthiourea derivatives by means of ^{1}H NMR spectroscopy.

Results and discussion

Synthesis of chiral bisthiourea derivatives 1–9 as CSAs.

Chiral bisthiourea derivatives **1**–**9** as chiral solvating agents were synthesized by the corresponding chiral diamines **10** with phenylisothiocyanate or its respective derivatives **11** in 55–67% yields (Scheme 1).[23] The detailed synthetic procedures are available in the ESI.

Synthesis of enantiomers of chiral amides 16–27 as guests.

First, enantiomers (*S*,*R*)-G**X** and (*R*,*S*)-G**X** (**X** = **16**–**24**) of amides with two stereogenic centers were prepared by an amidation reaction of (*S*)- and (*R*)-*N*-Ts-α-amino acids **12** and corresponding (*R*)- and (*S*)-amines **13** containing an amino acid residue, respectively (Scheme 2).[23a–c,24]

To evaluate the chiral discriminating capabilities of CSAs **1**–**9**, nine samples of (±)-G**16** were first prepared in the presence of CSAs **1**–**9** (molar ratio = 1:1, [(±)-G**16**] = 5 mM) in $CDCl_3$, respectively. Their ^{1}H NMR spectra were recorded on a 400 MHz NMR spectrometer. The results show that two enantiomers of (±)-G**16** can be clearly discriminated by the split ^{1}H NMR signals of the corresponding protons of various groups in the presence of CSAs **1**–**9**. The preliminary results indicate that CSAs **1**–**9** possess more sensitive and effective chiral discriminating capabilities towards enantiomers of (±)-G**16**. Subsequently, ^{1}H NMR spectra of enantiomers (*S*,*R*)-G**16** and (*R*,*S*)-G**16** with CSAs **1**–**9** (molar ratio = 1:1, [(*S*,*R*)-G**16**] = [(*R*,*S*)-G**16**] = 2.5 mM) were recorded in $CDCl_3$, respectively. The assignment of enantiomers of (±)-G**16** was easily determined by comparing the ^{1}H NMR signals and chemical shift values with the corresponding split protons. The number

of protons of the split ^{1}H NMR signals of enantiomers of (±)-G**16** and the maximum nonequivalent chemical shift values ($\Delta\Delta\delta$) are summarized in Fig. 1.

As shown in Fig. 1, CSAs **7**, **8** and **9** with a trifluoromethyl group on the phenyl ring exhibit superior chiral discriminating capabilities towards (±)-G**16** by comparison to other CSAs (**1**–**6**). For example, the split ^{1}H NMR signals of eight types of protons of (±)-G**16** were observed in the presence of CSA **7**, and their $\Delta\Delta\delta$ values are found to be 0.025 and 0.006 (CH(CH_3)$_2$), 0.058 (CH_3(Ala)), 0.054 (CH_3(Ts)), 0.069 (α-*H*(Val)), 0.191 (Ts*NH*), 0.038 (Ar*H*), and 0.184 (CO*NH*Ph) ppm, respectively. Among them, $\Delta\Delta\delta$ values of *NH* protons of Ts*NH* and CO*NH*Ph groups exceed 0.1 ppm (0.191 and 0.184 ppm), featuring better baseline resolution and absence of any overlaps (Fig. 2).

In order to obtain better chiral discriminating conditions, such as a better baseline resolution and more clearly split ^{1}H NMR signals with as fewer overlapping peaks as possible, several chiral discriminating conditions were tested. First, samples of (±)-G**16** with CSA **7** were prepared in different deuterated solvents, including $CDCl_3$, $CDCl_3/C_6D_6$ (5%), $CDCl_3/CD_3COCD_3$ (5%), $CDCl_3/CD_3OD$ (5%), and $CDCl_3$/DMSO-d_6 (5%). Their ^{1}H NMR spectra were measured on a 400 MHz spectrometer at room temperature. The $\Delta\Delta\delta$ values of the corresponding protons of CH_3 (Ts), Ts*NH* and CO*NH*Ph groups of (±)-G**16** in different deuterated solvents are summarized in Table 1.

As shown in Table 1, the intermolecular interaction between CSA **7** and (±)-G**16** were weakened ($CDCl_3/CD_3COCD_3$ (5%)), and even disappeared ($CDCl_3/CD_3OD$ (5%) or DMSO-d_6 (5%)) upon enhancement of solvent polarity. The $\Delta\Delta\delta$ values of the related protons of (±)-G**16** are slightly better in $CDCl_3/C_6D_6$ (5%). Based on these results, $CDCl_3$ alone, as a commonly used deuterated solvent, is more suitable for chiral recognition by ^{1}H NMR spectroscopy.

Subsequently, to explore the effects of concentration on chiral recognition, samples of (±)-G**16** with various concentrations (1, 2, 5 and 10 mM) were prepared in the presence of CSA **7** (molar ratio 1:1) in $CDCl_3$, and their ^{1}H NMR spectra were measured on a 400 MHz spectrometer at room temperature. The overlaid ^{1}H NMR spectra of protons of CH_3 (Ts) and CO*NH*Ph of (±)-G**16** are shown in Fig. 3.

As shown in Fig. 3, the results show that the $\Delta\Delta\delta$ values of the protons of the CH_3 (Ts) group of (±)-G**16** exhibit an increasing trend from 0.020 (1 mM) to 0.062 ppm (10 mM) as the concentration gradually increases. Similarly, the $\Delta\Delta\delta$ values of the *NH* proton of the CO*NH*Ph group of (±)-G**16** are also observing the same trend. Based on (i) the solubility of amides and CSAs, (ii) the general requirements for concentration in ^{1}H NMR spectroscopy, and (iii) the more clear display of the separated ^{1}H NMR signals, a concentration of 5 mM was deemed to be optimal and used in most cases.

Finally, samples of (±)-G**16** and CSA **7** with different molar ratios, including 1:3, 1:2, 1:1, 2:1 and 3:1, were prepared at a constant concentration (5 mM) of (±)-G**16** in $CDCl_3$, and their ^{1}H NMR spectra were recorded on a 400 MHz spectrometer at room temperature. The results show that the $\Delta\Delta\delta$ values of the protons of CH_3 (Ts) of (±)-G**16** were gradually

increasing as CSA **7** increased from 0.029 (3:1) to 0.053 ppm (1:3). Similarly, the $\Delta\Delta\delta$ values of the *NH* proton of CO*NH*Ph group of (±)-G**16** were also gradually increasing from 0.087 (3:1) to 0.298 ppm (1:3). Their overlaid ^{1}H NMR spectra and $\Delta\Delta\delta$ values of the protons of CH_3 (Ts) and *NH* of CO*NH*Ph groups of (±)-G**16** are shown in Fig. 4.

Based on (i) the solubility of amides and CSAs in different ratios, (ii) the more clearly separated ^{1}H NMR signals, and (iii) the more appropriate $\Delta\Delta\delta$ values, an 1:1 molar ratio of (±)-G**16**–G**27** with CSAs **1**–**9** was used for chiral recognition.

To further explore chiral recognition of other amides in the presence of CSAs **1**–**9** under the optimized chiral discriminating conditions, 99 samples of (±)-G**17**–G**27** were prepared in the presence of CSAs **1**–**9**, respectively, and their ^{1}H NMR spectra were recorded on a 400 MHz spectrometer. The split ^{1}H NMR signals of the related protons of 86 samples were distinctly observed in their spectra. For the remaining 13 samples, the split ^{1}H NMR signals cannot be clearly detected. The assignments of enantiomers of the differentiated samples were achieved in the manner noted above. Similarly, CSAs **7**, **8** and **9** show excellent chiral discriminating capabilities towards amides (±)-G**17**–G**27** ($\Delta\Delta\delta$, up to 0.407 ppm), presumably due to the presence of the 3, 5-trifluoromethyl moieties (CF_3) as a strong electron-withdrawing group, increase the ΔΔδ values, by resulting in an increasing in the acidity of NH proton of the thiourea group. The $\Delta\Delta\delta$ values of representative protons of (±)-G**16**–G**27** in the presence of CSAs **7**, **8** and **9**, along with their partial ^{1}H NMR spectra, are summarized in Table 2.

The $\Delta\Delta\delta$ values of the split protons of (±)-G**16**–G**27** in the presence of CSAs **1**–**9**, with the exception of $\Delta\Delta\delta$ values of the representative protons in the presence of CSAs **7**–**9**, are summarized in Table 3. In addition, their spectra are available in the ESI.

To further evaluate any underlying intermolecular interactions, theoretical calculations of enantiomers (*S*,*R*)-G**16** and (*R*,S)-G**16** with CSA **7**, as a representative example, were carried out by the hybrid density functional theory (B3LYP)/6–31G, respectively.[26] The proposed models show that the intermolecular hydrogen bonds were formed between CSA **7** with (*S*,*R*)-G**16** (CONH(Ph)···OCNH (2.061 Å), $(CH_3)_2$CH(NH)CO···NHCS (2.259 Å and 4.094 Å)), and (*R*,S)-G**16** (CONH(Ph)···OCNH (1.955 Å), $(CH_3)_2$CH(NH)CO···NHCS (2.377 Å and 4.232 Å)), respectively (Fig. 6).

As shown in Fig. 5, (*S*,*R*)-G**16** and (*R*,S)-G**16** with CSA **7** formed three intermolecular hydrogen bonds, respectively. The results exhibit that (*S*,*R*)-G**16** and (*R*,S)-G**16** with CSA **7** may form differential tight diastereomeric complexes according to the number and distances of their hydrogen bonds on the whole.

In addition, the calculated δ values of *NH* proton (CONHPh group) of (*S*,*R*)-G**16** and (*R*,*S*)-G**16** in the presence of CSA **7** were obtained according to the above theoretically calculated models, and were shown to be in keeping with the observed values (Table 5).

To investigate the behavior of intermolecular interactions, Job plots of (*S*,*R*)-G**16** and (*R*,*S*)-G**16** were constructed in the presence of CSA **7**. The Job plots of (±)-G**16** showed a maximum value ($X^*\Delta\delta$ = 0.069 ppm, $X^*\Delta\delta = X^*\Delta\delta_{(S,R)\text{-G}\mathbf{16}} - X^*\Delta\delta_{(R,S)\text{-G}\mathbf{16}}$ = 0.054 –

(–0.015)) at a molar fraction of $X = 0.5$, which suggests that a pair of diastereoisomeric complexes with 1:1 stoichiometry was established between (*S,R*)-G**16** and (*R,S*)-G**16** with CSA **7**, respectively. Among them, To further verify the above results, Job plots of (*S,R*)-G**17** and (*R,S*)-G**17** were carried out in the presence of CSA **8**. The similar results (1:1 complexes) were obtained because a maximum value ($X^*\Delta\delta = 0.041$ ppm, $X^*\Delta\delta = X^*\Delta\delta_{(S,R)\text{-G}\mathbf{17}} - X^*\Delta\delta_{(R,S)\text{-G}\mathbf{17}} = 0.025 - (-0.016)$) was observed at a molar fraction of $X = 0.5$ (Fig 5).

To evaluate the strength of intermolecular noncovalent interactions, the binding constants (K_a) for (*S,R*)-G**16** and (*R,*S)-G**16** with CSA **7** were determined by ^{1}H NMR titrations. The K_a values were calculated by means of the nonlinear curve-fitting method, respectively.[25] Detailed results are summarized in Table 4.

Now that CSAs **1**–**9** have been established to demonstrate excellent chiral discriminating capabilities towards amides **16**–**27**, to further explore their practical application in determining enantiomeric excess (ee), 7 samples containing (*S,R*)-G**16** with 90%, 85%, 65%, 45%, 25%, 10%, 0% ee were prepared in the presence of CSA **7** in $CDCl_3$, and their ^{1}H NMR spectra were recorded on a 400 MHz NMR spectrometer. Enantiomeric excess for all samples were accurately calculated based on the integration of the *NH* proton of the CO*NH*Ph groups, featuring well-separated ^{1}H NMR signals of (*S,R*)-G**16** and (*R,*S)-G**16** (up to 90% ee) (Fig. 7 (a)). Excellent linear correlations between the theoretical (*X*) and observed (*Y*) ee% values were obtained in the presence of CSA **7** (Fig. 7 (c)). To further verify the practical applicability in determining ee values, another set of samples containing (*S,R*)-G**16** with 85%, 65%, 45%, 25%, 10%, 0% ee was also prepared in the presence of CSA **8** in $CDCl_3$, and their ^{1}H NMR spectra were measured (Fig. 7 (b)). The linear correlations between the theoretical (*X*) and observed (*Y*) ee% values were obtained in the presence of CSA **8** (Fig. 6 (7)).The results obtained proved to be accurate and feasible.

Conclusions

In summary, enantiomers of amides **16**–**27** with two stereogenic centers were prepared from the corresponding *D*- and *L*-α-amino acids as initial chiral sources for chiral recognition by ^{1}H NMR spectroscopy. Enantiomers of amides **16**–**27** were successfully differentiated in the presence of CSAs **1**–**9** by ^{1}H NMR spectroscopy. Most importantly, during the execution of this study, CSAs **7**–**9** with 3,5-trifluoromethyl moieties as a strong electron-withdrawing group, were shown to exhibit highly sensitive and effective chiral discriminating capabilities towards these chiral amides, leading to a better baseline resolution, larger nonequivalent shift values and multiple detection windows. The Job plots of (*S,R*)-G**16** and (*R,S*)-G**16** with CSA **7**, and (*S,R*)-G**17** and (*R,S*)-G**17** with CSA **8** were carried out, respectively. The association constants (K_a) of (*S,R*)-G**16** and (*R,S*)-G**16** with CSA **7** were evaluated. Theoretical calculations of enantiomers of (±)-G**16** with CSA **7** were performed by means of the hybrid density functional theory (B3LYP) with the standard basis sets of 3–21G of the Gaussian 03 program. Enantiomeric excesses (ee) of G**16** with different optical compositions (up to 90% ee) were calculated based on the integrations of ^{1}H NMR signals of the split NH proton (CO*NH*Ph group) of G**16** in the presence of CSAs **7** and **8**, respectively, giving excellent and accurate experimental results, in agreement with

theoretical data. In conclusion, a practical strategy for chiral recognition of amides with two stereogenic centers has been effectively established in the presence of CSAs **1**–**9** by using ^{1}H NMR spectroscopy.

Supplementary Material

Refer to Web version on PubMed Central for supplementary material.

Acknowledgements

This work was supported by Scientific Research Fund Performance Award of Beijing Normal University (Award number 10200/111203277). Work in the Missouri Lab (P. S.) is supported by the National Institute of General Medical Science of the National Institutes of Health under Award Numbers R15GM117508 and R15GM139071.

Notes and references

1. (a)Fabro S, Smith RL and Williams RT, Nature, 1967, 215, 296; [PubMed: 6059519] (b)Mane S, Anal. Methods, 2016, 8, 7567;(c)Calcaterra A. and D'Acquarica I, J. Pharm. Biomed. Anal. 2018, 147, 323. [PubMed: 28942107]
2. (a)Pirkle WH and Pochapsky TC, Chem. Rev, 1989, 89, 347;(b)Zhang JY, Sun JY, Liu YR, Yu J. and Guo XJ, Chromatographia, 2019, 82, 649;(c)Payne C. and Kass SR, Chemistryselect, 2020, 5, 1810.
3. (a)Parker D, Chem. Rev, 1991, 91, 1441;(b)Li GW, Cao JM, Zong W, Lei XX and Tan RX, Org. Chem. Front, 2016, 3, 96;(c)Yang L, Wenzel T, Williamson RT, Christensen M, Schafer W. and Welch CJ, ACS Cent. Sci, 2016, 2, 332; [PubMed: 27280168] (d)Jang S. and Kim H, iScience, 2019, 19, 425. [PubMed: 31421597]
4. (a)Nieto S, Lynch VM, Anslyn EV, Kim H. and Chin J, Org. Lett, 2008, 10, 5167; [PubMed: 18939802] (b)Pilicer SL and Wolf C, J. Org. Chem, 2020, 85, 11560.
5. (a)Guo JH, Wu JY, Siuzdak G. and Finn MG, Angew. Chem. Int. Ed, 1999, 38, 1755;(b)Faggi E, Vicent C, Luis SV and Alfonso I, Org. Biomol. Chem, 2015, 13, 11721;(c)Wang L, Jin Z, Wang XY, Zeng S, Sun CR and Pan YJ, Anal. Chem, 2017, 89, 11902.
6. Gropp C, Husch T, Trapp N, Reiher M. and Diederich F, Angew. Chem. Int. Ed, 2018, 57, 16296.
7. (a)Demirtas HN, Bozkurt S, Durmaz M, Yilmaz M. and Sirit A, Tetrahedron, 2009, 65, 3014;(b)De los Santos ZA, Lynch CC and Wolf C, Angew. Chem. Int. Ed, 2019, 58, 1198;(c)Akdeniz A, Minami T, Watanabe S, Yokoyama M, Ema T. and Jr PA, Chem. Sci, 2016, 7, 2016;(d)Zhu YY, Wu XD, Abed M, Gu SX and Pu L, Chem. Eur. J, 2019, 25, 7866. [PubMed: 30893491]
8. (a)Lakshmipriya A, Chaudhari SR and Suryaprakash N, Chem. Commun, 2015, 51, 13492;(b)Virgili A, Granados A, Jaime C, Suárez-López R, Parella T. and Monteagudo E, J. Org. Chem, 2020, 85, 7247. [PubMed: 32401518]
9. (a)Chaughari SR and Suryaprakash N, J. Org. Chem, 2012, 77, 648; [PubMed: 22145800] (b)Seco JM, Quiñoá E. and Riguera R, Chem. Rev, 2012, 112, 4603; [PubMed: 22658125] (c)Kriegelstein M, Profous D, Přibylka A. and Cankař P, J. Org. Chem, 2020, 85, 12912.
10. (a)Bian GL, Fan HJ, Huang HY, Yang SW, Zong H, Song L. and Yang GJ, Org. Lett, 2015, 17, 1369; [PubMed: 25751415] (b)Cuřínová P, Hájek P, Janků K. and Holakovský R, Chirality, 2019, 31, 410; [PubMed: 30920055] (c)Seo M-S, Jang S. and Kim H, 2018, 54, 6804;(b)Alimohammadi M, Hasaninejad A, Luu QH and Gladysz JA, J. Org. Chem, 2020, 85, 11250.
11. (a)Benson SC, Cai P, Colon M, Haiza MA, Tokles M. and Snyder JK, J. Org. Chem, 1988, 53, 5335;(b)Sun ZF, Chen ZX, Wang YQ, Zhang XB, Xu J, Bian GL and Song L, Org. Lett, 2020, 22, 589. [PubMed: 31913635]
12. (a)Yang K, Li SZ, Wang YH, Zhang WZ, Xu ZH, Zhou XY, Zhu RX, Luo J. and Wan Q, RSC Adv, 2014, 4, 6517;(b)Yang J, Chatelet B, Dufaud V, Hérault D, Jean M, Vanthuyne N, Mulatier J-C, Pitrat D, Guy L, Dutasta J-P and Martinez A, Org. Lett, 2020, 22, 891. [PubMed: 31985232]

13. (a)Wolf C, Cook AM and Dannatt JE, Tetrahedron: Asymmetry, 2014, 25, 163;(b)Bian GL, Yang SW, Huang HY, Zong H, Song L, Fan HJ and Sun XQ, Chem. Sci, 2016, 7, 932. [PubMed: 29899892]

14. (a)Bai LW, Chen P, Xiang JX, Sun JR and Lei XX, Org. Biomol. Chem, 2019, 17, 1466; [PubMed: 30672950] (b)Malinowska M, Jarzyński S, Pieczonka A, Rachwalski M, Leśniak S. and Zawisza A, J. Org. Chem, 2020, 85, 11794.

15. (a)Jang S. and Kim H, Org. Lett, 2020, 22, 4185. [PubMed: 32396379]

16. (a)Shirbhate ME, Nandhakumar R, Kim Y, Kim S-J, Kim SK and Kim KM, Eur. J. Org. Chem, 2018, 4959;(b)Recchimurzo A, Micheletti C, Uccello-Barretta G. and Balzano F, J. Org. Chem, 2020, 85, 5342. [PubMed: 32191037]

17. Faggi E, Vicent C, Luis SV and Alfonso I, Org. Biomol. Chem, 2015, 3, 11721.

18. (a)He X, Zhang M, Guo Y-Y, Mao X-M, Chen X–A and Li Y-Q, Org. Lett, 2018, 20, 6323; [PubMed: 30277789] (b)Wen K-G, Peng Y-Y and Zeng X-P, Org. Chem. Front, 2020, 7, 2576.

19. (a)Fabro S, Smith r. l. and Williams RT, Nature, 1967, 215, 196; [PubMed: 6049121] (b)Yang X, Zhao Y, Hsieh M-T, Xin G, Wu R-T, Hsu P-L, Horng L-Y, Sung H-C, Cheng C-H and Lee K-H, J. Nat. Prod, 2017, 80, 3284; [PubMed: 29164880]

20. (a)de Figueiredo RM, Suppo J-S and Campagne J-M, Chem. Rev, 2016, 116, 12029;(b)Santos AS, Silva AMS and Marques MMB, Eur. J. Org. Chem, 2020, 2501.

21. (a)Crespo L, Sanclimens G, Pons M, Giralt E, Royo M. and Albericio F, Chem. Rev, 2005, 105, 1663; [PubMed: 15884786] (b)Pattabiraman VR and Bode JW, Nature, 2011, 480, 471. [PubMed: 22193101]

22. (a)Brown DG and Boström J, J. Med. Chem, 2016, 59, 4443; [PubMed: 26571338] (b)Song WZ, Dong K. and Li M, Org. Lett, 2020, 22, 371. [PubMed: 31742411]

23. (a)Dahiya R, Pak. J. Pharm. Sci, 2007, 20, 317; [PubMed: 17604256] (b)Li JY, Li X, Zhou PX, Zhang L, Luo SZ and Cheng J-P, Eur. J. Org. Chem, 2009, 4486;(c)Curini M, Epifano F, Maltese F. and Marcotullio MC, Tetrahedron Lett, 2002, 43, 3821;(d)Fotaras S, Kokotos CG, Tsandi E. and Kokotos G, Eur. J. Org. Chem, 2011, 1310.

24. Ghosh D, Sahu D, Saravanan S, Abdi SHR, Ganguly B, Khan NH, Kureshy RI and Bajaj HC, Org. Biomol. Chem, 2013, 11, 3451. [PubMed: 23411590]

25. (a)Fielding L, Tetrahedron, 2000, 56, 6151.(b)Schulz N, Schindler S, Huber SM and Erdelyi M, J. Org. Chem, 2018, 83, 10881.

26. Becke AD, J. Chem. Phys. 1993, 98, 5648.

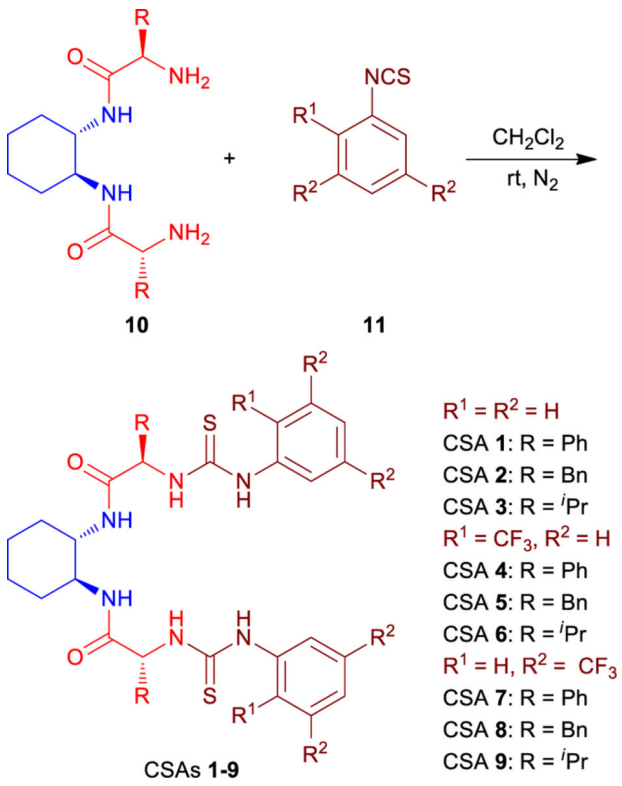

Scheme 1.

Synthesis of chiral bisthiourea derivatives **1**–**9**.

CSAs **1**–**9** were characterized by ^{1}H NMR, ^{13}C NMR, ^{19}F NMR (CSAs **4**–**9**), and IR spectroscopies, and by HRMS methods, and their spectra or data are available in the ESI. As shown in Scheme 1, the outstanding features of CSAs **1**–**9** rely on the presence of two thiourea units and two amide groups, as potential multiple hydrogen bonding sites with chiral substrates, to facilitate formation of diastereomeric complexes for chiral recognition by ^{1}H NMR spectroscopy.

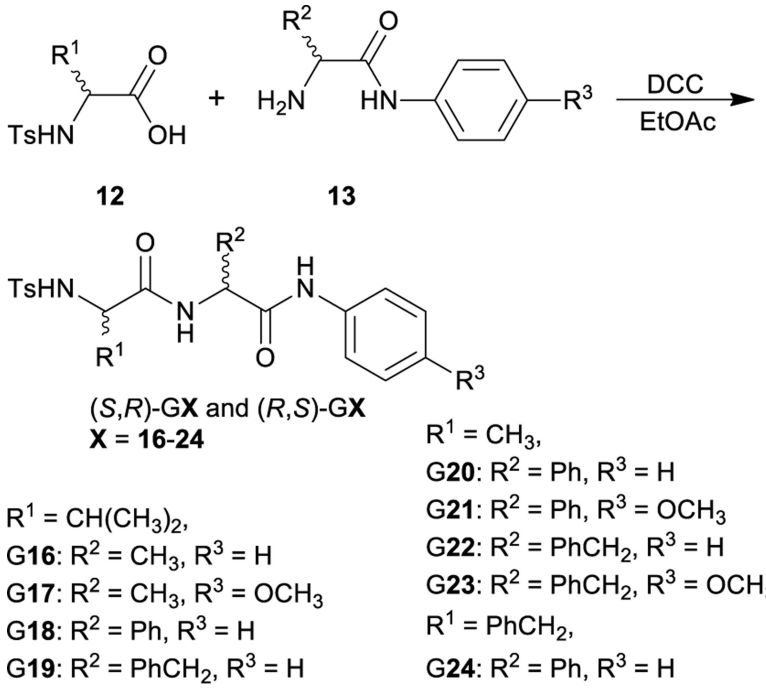

Scheme 2.

Synthesis of enantiomers of chiral amides **16**–**24**.

In addition, enantiomers (*S*,*R*)-G**X** and (*R*,*S*)-G**X** (**X** = **25**–**27**) of amides with two stereogenic centers were derived from (*S*)- and (*R*)-*N*-Ts-Pro **14** with (*R*)- and (*S*)-amines **15** according to the aforementioned synthetic procedure (Scheme 3).

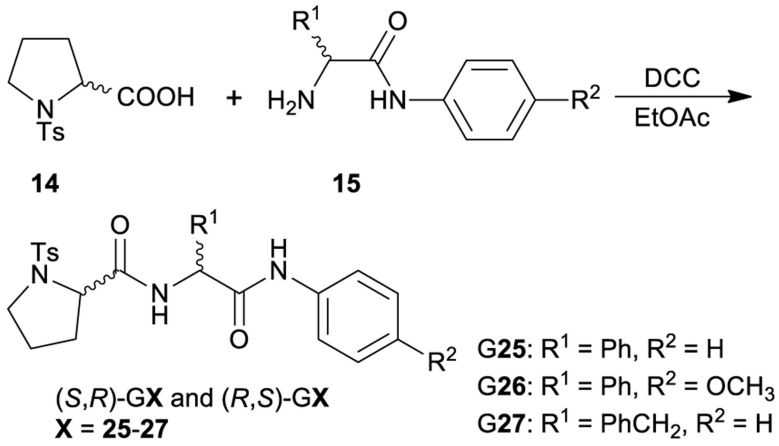

Scheme 3.

Synthesis of enantiomers of chiral amides **25**–**27**.

The structures of all enantiomers (*S*,*R*)-G**X** and (*R*,*S*)-G**X** (**X** = **16**–**27**) were characterized by ^{1}H NMR, ^{13}C NMR, IR and HRMS. In addition, ^{1}H-^{1}H COSY and ^{1}H-^{13}C HSQC spectra of (*S*,*R*)-G**X** or (*R*,*S*)-G**X** were measured for the correct assignment of the related protons of CO*NH* and Ts*NH* groups of amides. The detailed procedures of synthesis of enantiomers of (±)-G**16**–**27**, along with their spectra, are available in the ESI.

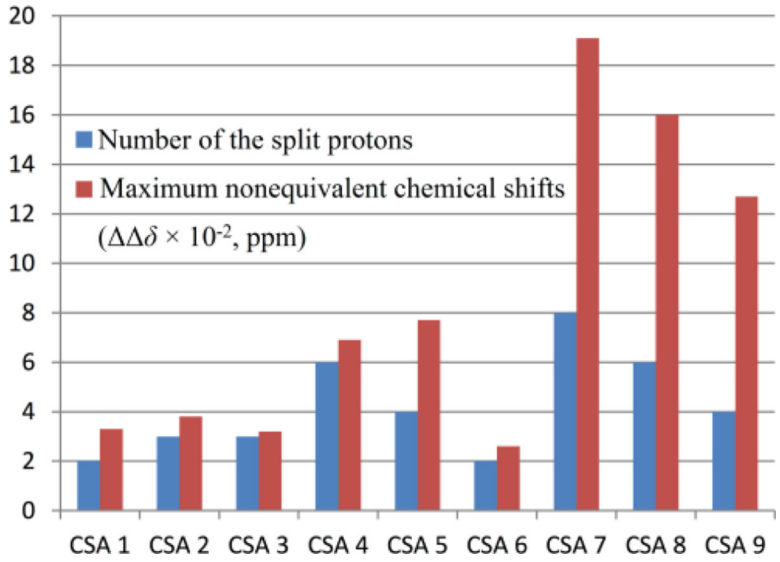

Fig. 1.

Number (■) of protons of the split ^{1}H NMR signals of (±)-G**16** and the maximum nonequivalent chemical shift values (■), ($\Delta\Delta\delta \times 10^{-2}$, ppm) in the presence of CSAs **1**–**9** (1:1, [(±)-G**16**] = 5 mM) in $CDCl_3$ (400 MHz) at room temperature, respectively. $\Delta\Delta\delta = |\Delta\delta_{(S,R)\text{-G}\mathbf{16}} - \Delta\delta_{(R,S)\text{-G}\mathbf{16}}|$, $\Delta\delta_{(S,R)\text{-G}\mathbf{16}} = \delta_{(S,R)\text{-}\mathbf{G16}} - \delta_{free}$, $\Delta\delta_{(R,S)\text{-G}\mathbf{16}} = \delta_{(R,S)\text{-G}\mathbf{16}} - \delta_{free}$.

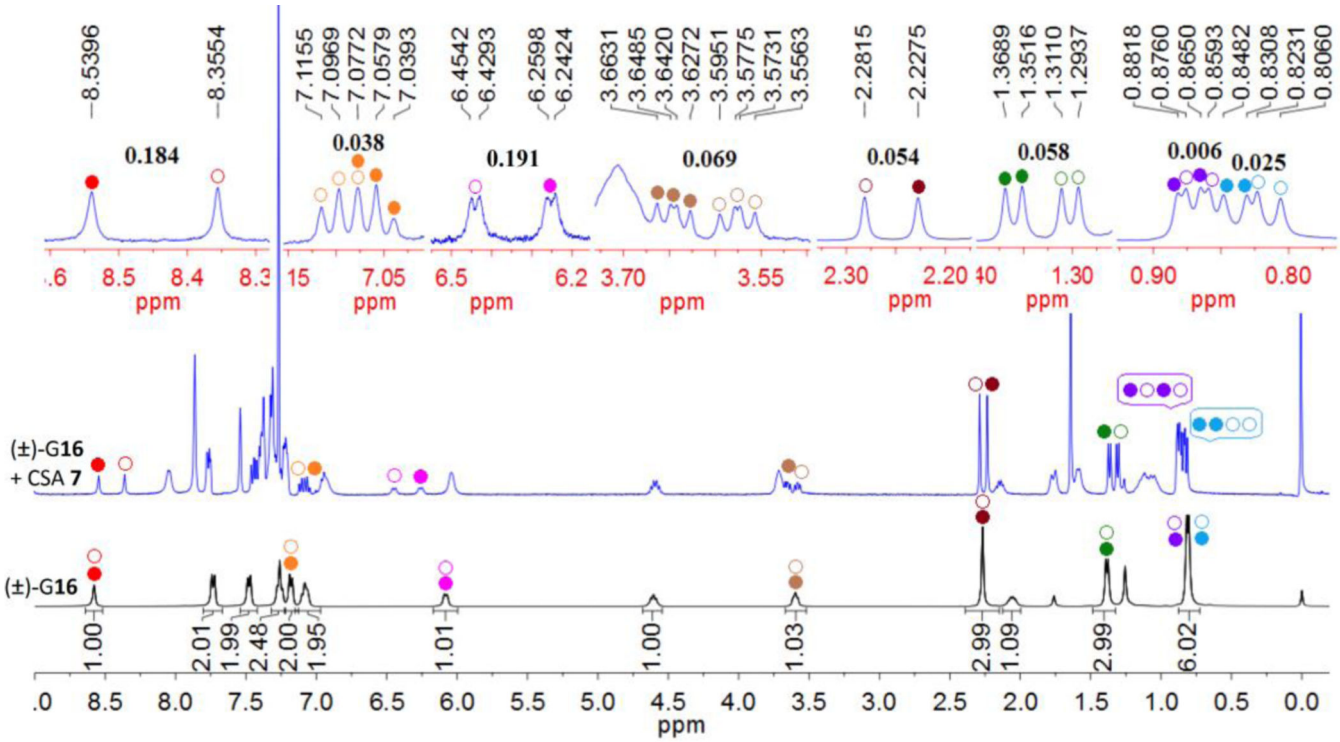

Fig. 2.

(a) ^{1}H NMR spectrum of (±)-G**16** in $CDCl_3$ at room temperature (400 MHz), ([(±)-G**16**] = 5 mM); (b) ^{1}H NMR spectrum of (±)-G**16** in the presence of CSA **7** (1:1, [(±)-G**16**] = 5 mM) in $CDCl_3$ at room temperature (400 MHz). Different colors marks "●" and "○" stand for different protons of the split ^{1}H NMR signals of (*S,R*)-G**16** and (*R,S*)-G**16**, respectively, $\Delta\Delta\delta = |\Delta\delta_{(S,R)\text{-G16}} - \Delta\delta_{(R,S)\text{-G16}}|$, $\Delta\delta_{(S,R)\text{-G16}} = \delta_{(S,R)\text{-G16}} - \delta_{free}$, $\Delta\delta_{(R,S)\text{-G16}} = \delta_{(R,S)\text{-G16}} - \delta_{free}$.

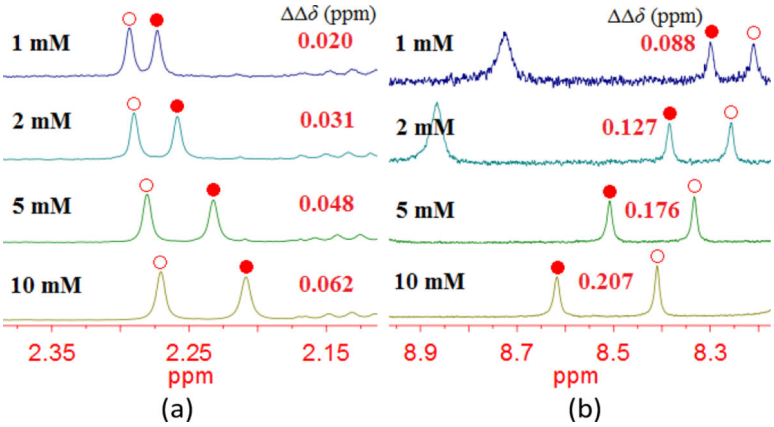

Fig. 3.

Overlaid ^{1}H NMR spectra of the protons of CH_3 (Ts) (a), and CONHPh (b) of (±)-G**16** with different concentrations in the presence of CSA **7** in $CDCl_3$ at room temperature (400 MHz).The molar ratio of (±)-G**16** and CSA **7** is 1:1, $\Delta\Delta\delta = |\Delta\delta_{(S,R)\text{-G}\mathbf{16}} - \Delta\delta_{(R,S)\text{-G}\mathbf{16}}|$, $\Delta\delta_{(S,R)\text{-G}\mathbf{16}} = \delta_{(S,R)\text{-G}\mathbf{16}} - \delta_{free}$, $\Delta\delta_{(R,S)\text{-G}\mathbf{16}} = \delta_{(R,S)\text{-G}\mathbf{16}} - \delta_{free}$.

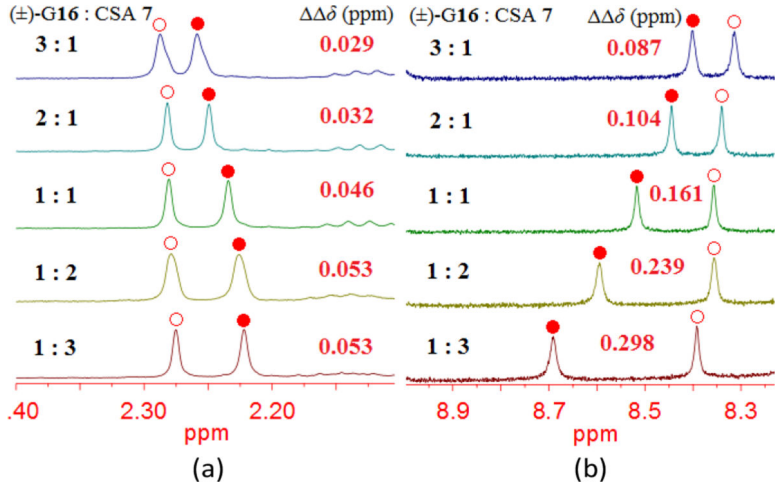

Fig. 4.

Overlaid ^{1}H NMR spectra of the protons of CH_3 (Ts) (a), and of *NH* of CO*NH*Ph (b) of (±)-G**16** with CSA **7** in different molar ratios (400 MHz).The concentration of (±)-G**16** is 5 mM in $CDCl_3$, unchangeable, $\Delta\Delta\delta = |\Delta\delta_{(S,R)\text{-G}\mathbf{16}} - \Delta\delta_{(R,S)\text{-G}\mathbf{16}}|$, $\Delta\delta_{(S,R)\text{-G}\mathbf{16}} = \delta_{(S,R)\text{-G}\mathbf{16}} - \delta_{free}$, $\Delta\delta_{(R,S)\text{-G}\mathbf{16}} = \delta_{(R,S)\text{-G}\mathbf{16}} - \delta_{free}$.

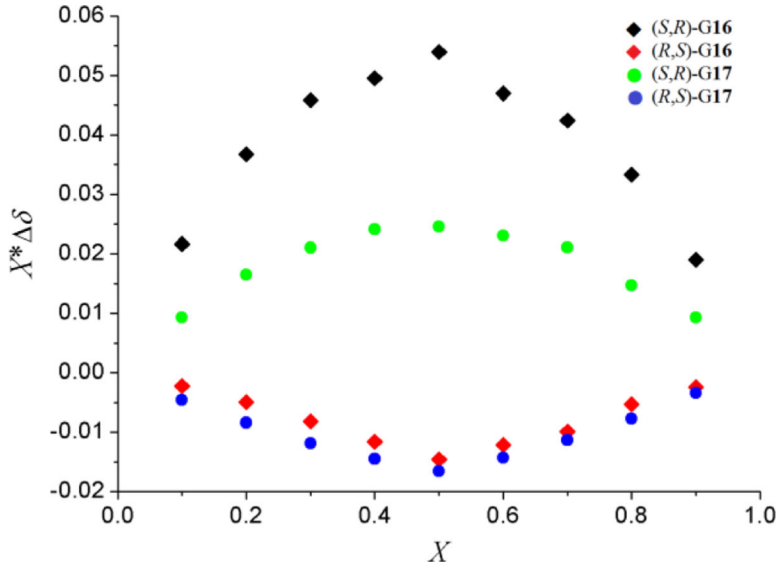

Fig. 5.

Job plots for complexes of (*S*,*R*)-G**16** and (*R*,*S*)-G**16** with CSA **7**, (*S*,*R*)-G**17** and (*R*,*S*)-G**17** with CSA **8**, respectively. Δδ stands for chemical shift change of the *NH* proton (CO*NH*Ph) of enantiomers of (±)-G**16** and G**17** in the presence of CSAs **7** and **8**, respectively. *X* stands for the molar fraction of enantiomers of (±)-G**16** and G**17**. $\Delta\delta = \delta_{(S,R)\text{-G16 or G17}} - \delta_{free}$. $\Delta\delta = \delta_{(R,S)\text{-G16 or G17}} - \delta_{free}$. The total concentration of enantiomers of (±)-G**16** with CSA **7** or (±)-G**17** with **8** was 5 mM, respectively.

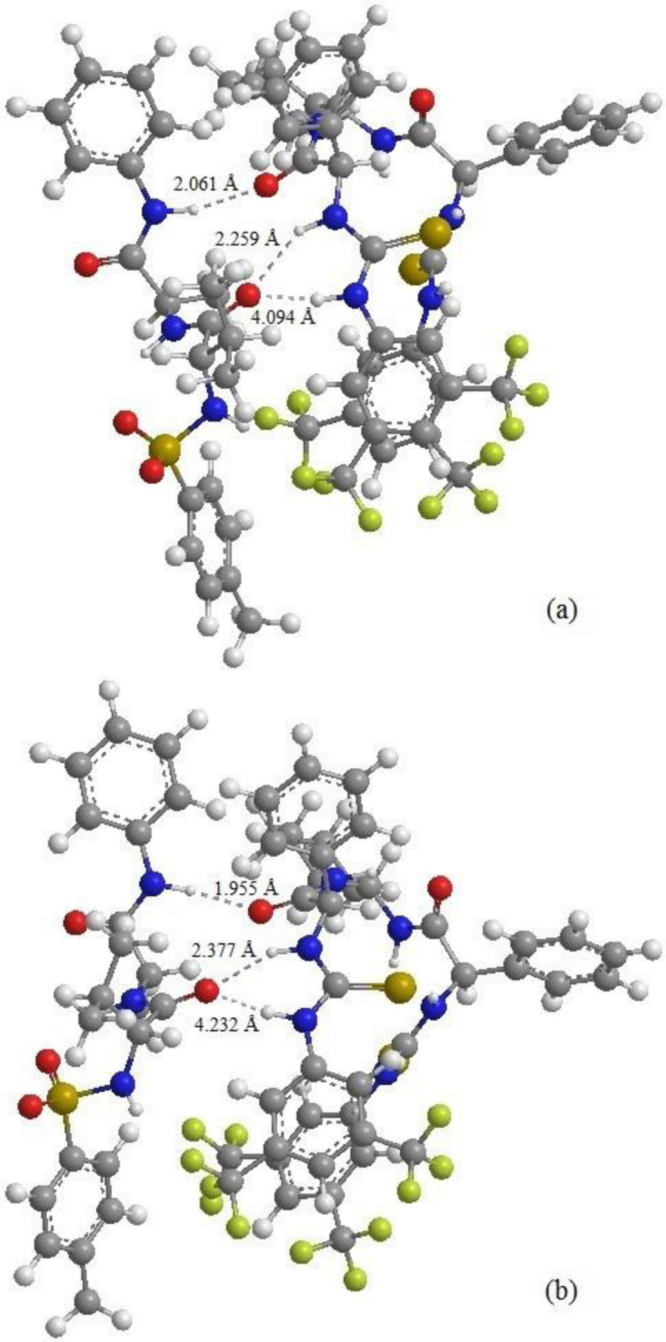

Fig. 6.

Propoded bonding models for the hydrogen bonding interactions between CSA **7** and enantiomers (*S*,*R*)-G**16** (a) and (*R*,S)-G**16** (b).

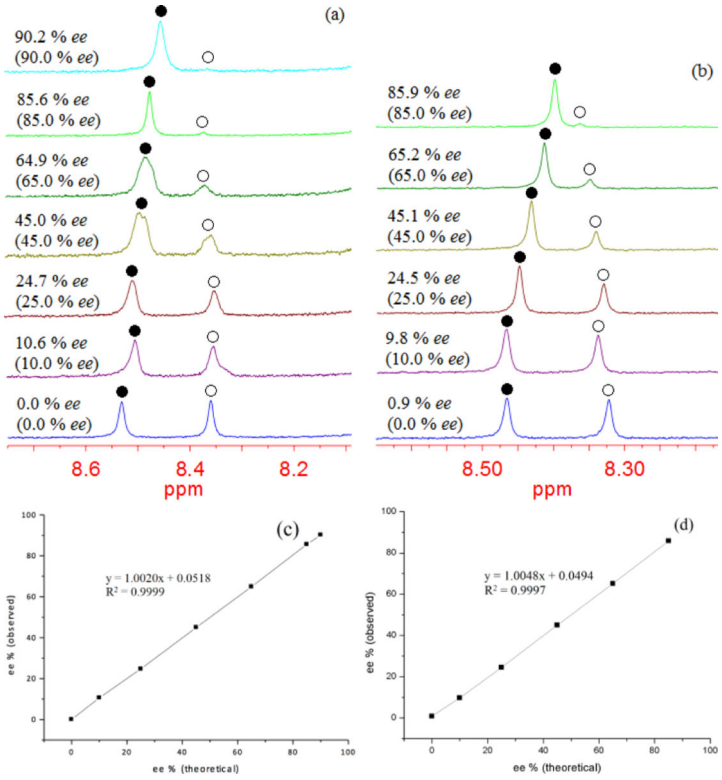

Fig. 7.

Determination of enantiomeric excesses of G**16**, *ee* (%) = [((*S*,*R*)-G**16** – (*R*,S)-G**16**))/((*S*,*R*)-G**16** + (*R*,S)-G**16**))]×100%, Overlaid ^{1}H NMR spectra of the *NH* proton of CO*NH*Ph group of (*S*,*R*)-G**16** (●) and (*R*,S)-G**16** (○) in the presence of CSAs **7** (a) and **8** (b), [**G16**] = 5 mM. Linear correlations between the theoretical (*X*) and observed (*Y*) *ee* % values of **G16** with CSAs **7** (c) and **8** (d), respectively. $\Delta\Delta\delta = |\Delta\delta_{(S,R)\text{-G}\mathbf{16}} - \Delta\delta_{(R,S)\text{-G}\mathbf{16}}|$, $\Delta\delta_{(S,R)\text{-G}\mathbf{16}} = \delta_{(S,R)\text{-G}\mathbf{16}} - \delta_{free}$, $\Delta\delta_{(R,S)\text{-G}\mathbf{16}} = \delta_{(R,S)\text{-G}\mathbf{16}} - \delta_{free}$.

Table 1.

Nonequivalent chemical shift values ($\Delta\Delta\delta$, ppm) of the related proton of (±)-G**16** in the presence of CSA **7** in different deuterated solvents at room temperature (400 MHz).

Solvent	CO*NH*Ph	Ts*NH*	CH_3(Ts)
$CDCl_3$	0.184	0.191	0.054
$CDCl_3/C_6D_6$ (5%)	0.189	0.173	0.048
$CDCl_3/CD_3COCD_3$ (5%)	0.042	0.090	0.011
$CDCl_3/CD_3OD$ (5%)	0.0	0.0	0.0
$CDCl_3$/DMSO-d_6 (5%)	0.0	0.0	0.0

[a](±)-G**16**/ CSA **7** = 1:1, [(±)-G**16**] = 5 mM, $\Delta\Delta\delta = |\Delta\delta(S,R)\text{-G}\mathbf{16} - \Delta\delta(R,S)\text{-G}\mathbf{16}|$, $\Delta\delta(S,R)\text{-G}\mathbf{16} = \delta(S,R)\text{-G}\mathbf{16} - \delta_{free}$, $\Delta\delta(R,S)\text{-G}\mathbf{16} = \delta(R,S)\text{-G}\mathbf{16} - \delta_{free}$.

Table 2.

Nonequivalent chemical shifts (ΔΔ*δ*, ppm) of the representative protons of (±)-G**16**–**G27** and their partial ^{1}H NMR spectra in the presence of CSAs **7**, **8** and **9** in $CDCl_3$ at room temperature, respectively (400 MHz).[a]

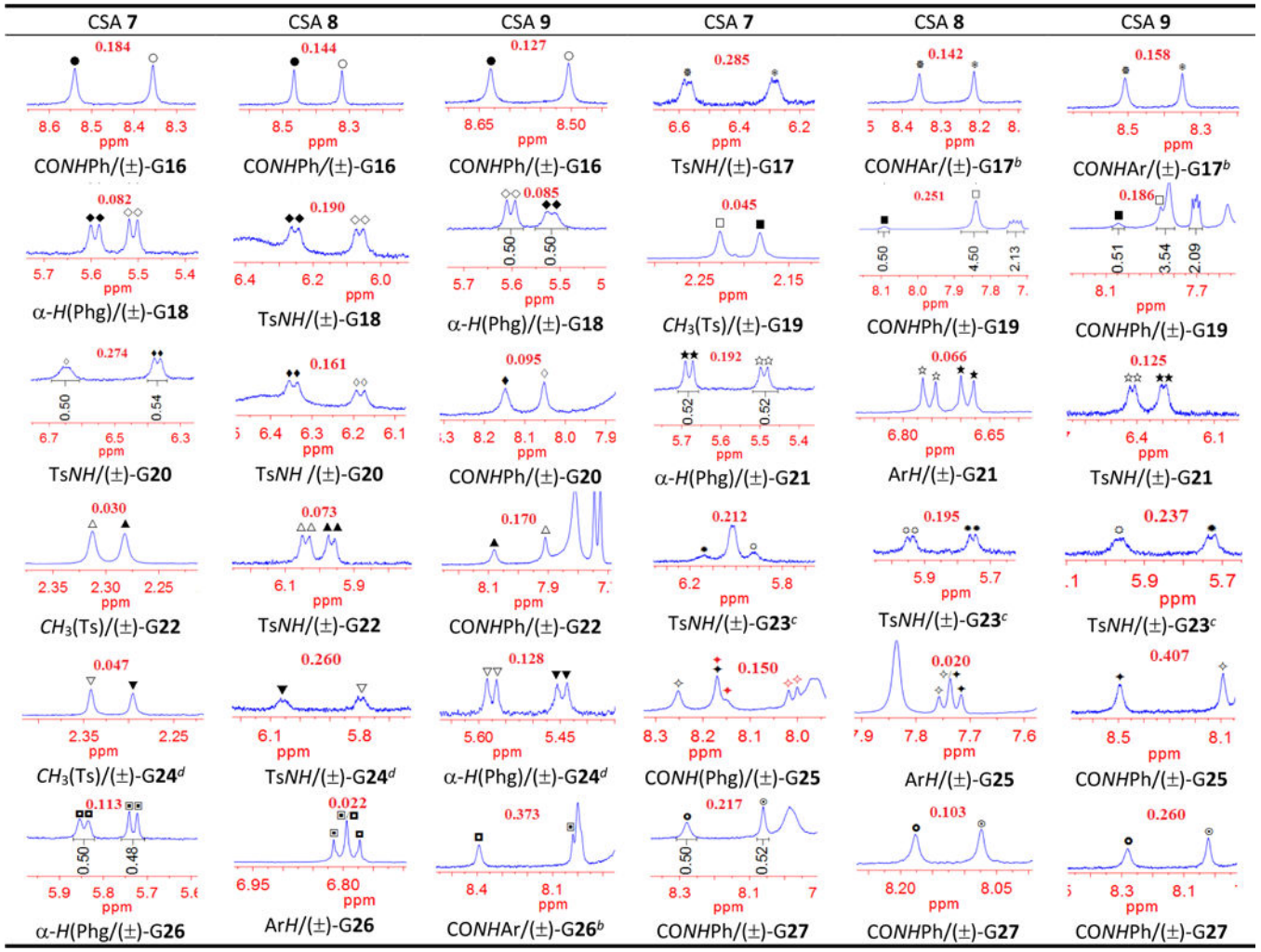

[a] Marks of different shapes "solid" and "hollow" (such as, ● and ○) stand for (*S,R*)-G**X** and (*R,S*)-G**X** (**X** = **16**–**27**), respectively. $\Delta\Delta\delta = |\Delta\delta_{(S,R)\text{-G}\mathbf{X}} - \Delta\delta_{(R,S)\text{-G}\mathbf{X}}|$, $\Delta\delta_{(S,R)\text{-G}\mathbf{X}} = \delta_{(S,R)\text{-G}\mathbf{X}} - \delta_{free}$, $\Delta\delta_{(R,S)\text{-G}\mathbf{X}} = \delta_{(R,S)\text{-G}\mathbf{X}} - \delta_{free}$. [Guest] = 5 mM, H:G = 1:1;

[b] Ar = 4-MeOC$_6$H$_4$;

[c] [Guest] = 4 mM;

[d] [Guest] = 2.5 mM.

Table 3.

Nonequivalent chemical shifts (ΔΔ*δ*, ppm) of (±)-G**16**–G**27** in the presence of CSAs **1**–**9** in $CDCl_3$ at room temperature, with the exception of the representative protons of (±)-G**16**–G**27** in the presence of CSAs **7**–**9** (400 MHz).[a]

Guest	CSA	Proton	ΔΔ*δ*	Guest	CSA	Proton	ΔΔ*δ*	Guest	CSA	Proton	ΔΔ*δ*
(±)-G**16**	CSA **1**	CO*NH*(Ala)	0.028			CO*NH*Ph	0.045		CSA **2**	CO*NH*(Phe)	0.039
		CO*NH*Ph	0.033	(±)-G**19**	CSA **1**	Ph*CH*$_2$	0.009			Ar*H*	0.005
	CSA **2**	*CH*$_3$(Ala)	0.006			CO*NH*Ph	0.030			CO*NH*Ar[b]	0.013
		CO*NH*(Ala)	0.036		CSA **2**	*CH*$_3$(Ts)	0.005		CSA **3**	*CH*$_3$(Ala)	0.003
		CO*NH*Ph	0.038			CO*NH*(Phe)	0.039			*CH*$_3$O	0.002
	CSA **3**	Ts*NH*	0.019			CO*NH*Ph	0.023			CO*NH*(Phe)	0.038
		CO*NH*(Ala)	0.022		CSA **3**	CO*NH*(Phe)	0.030			Ar*H*	0.006
		CO*NH*Ph	0.032			CO*NH*Ph	0.020			CO*NH*Ar[b]	0.014
	CSA **4**	*CH*$_3$(Val)	0.017		CSA **4**	*CH*$_3$(Ts)	0.009		CSA **4**	*CH*$_3$O	0.016
		CH$_3$(Ala)	0.004			Ph*CH*$_2$	0.004			Ts*NH*	0.027
		Ts*NH*	0.038			α-*H*(Phe)	0.004			CO*NH*(Phe)	0.116
		CO*NH*(Ala)	0.069			CO*NH*(Phe)	0.097			Ar*H*	0.030
		Ar*H*	0.018			Ar*H*	0.018		CSA **5**	*CH*$_3$(Ts)	0.008
		CO*NH*Ph	0.048		CSA **5**	*CH*$_3$(Ts)	0.014			*CH*$_3$O	0.010
	CSA **5**	*CH*$_3$(Ts)	0.010			CO*NH*(Phe)	0.083		CSA **7**	*CH*$_3$(Ala)	0.042
		Ts*NH*	0.008		CSA **6**	CO*NH*(Phe)	0.029			*CH*$_3$(Ts)	0.024
		CO*NH*(Ala)	0.077		CSA **7**	α-*H*(Val)	0.050			*CH*$_3$O	0.014
		CO*NH*Ph	0.055		CSA **8**	*CH*$_3$(Val)	0.031			Ar*H*	0.056
	CSA **6**	CO*NH*(Ala)	0.026			*CH*$_3$(Val)	0.049		CSA **8**	*CH*$_3$(Ala)	0.020
		CO*NH*Ph	0.019			*CH*$_3$(Ts)	0.009			*CH*$_3$(Ts)	0.029
	CSA **7**	*CH*$_3$(Val)	0.025			α-*H*(Val)	0.095			*CH*$_3$O	0.008
		CH$_3$(Val)	0.006			Ts*NH*	0.097			Ar*H*	0.045
		CH$_3$(Ala)	0.058		CSA **9**	*CH*$_3$(Ts)	0.020		CSA **9**	*CH*$_3$(Ala)	0.011
		CH$_3$(Ts)	0.054			Ts*NH*	0.104			*CH*$_3$(Ts)	0.022
		α-*H*(Val)	0.069			Ar*H*	0.017			Ph*CH*$_2$	0.082

Guest	CSA	Proton	ΔΔ*δ*	Guest	CSA	Proton	ΔΔ*δ*	Guest	CSA	Proton	ΔΔ*δ*
		Ts*NH*	0.191			Ar*H*	0.017			*CH*$_3$O	0.009
		Ar*H*	0.038	(±)-G**20**	CSA **1**	Ts*NH*	0.057			α-*H*(Phe)	0.076
	CSA **8**	*CH*$_3$(Ala)	0.020		CSA **2**	α-*H*(Phg)	0.006			Ar*H*	0.028
		CH(CH$_3$)$_2$	0.059			Ts*NH*	0.032			Ar*H*	0.005
		CH$_3$(Ts)	0.017		CSA **3**	Ar*H*	0.005	(±)-G**24**[d]	CSA **1**	Ts*NH*	0.058
		α-H(Ala)	0.036		CSA **4**	α-*H*(Phg)	0.010			α-*H*(Phg)	0.019
		Ts*NH*	0.160			Ts*NH*	0.088		CSA **4**	Ts*NH*	0.098
	CSA **9**	*CH*$_3$(Ala)	0.035			CO*NH*(Phg)	0.044			α-*H*(Phg)	0.038
		CH$_3$(Ts)	0.009		CSA **5**	α-*H*(Phg)	0.005		CSA **5**	Ts*NH*	0.055
		α-H(Val)	0.043			Ts*NH*	0.030		CSA **7**	α-*H*(Phg)	0.042
(±)-G**17**	CSA **1**	*CH*$_3$(Ala)	0.005		CSA **7**	*CH*$_3$(Ts)	0.036			Ar*H*	0.028
		CO*NH*(Ala)	0.028			α-*H*(Phg)	0.135		CSA **8**	Ph*CH*$_2$	0.026
	CSA **2**	CO*NH*(Ala)	0.034			Ar*H*	0.034			α-*H*(Phe)	0.056
		Ar*H*	0.006		CSA **8**	*CH*$_3$(Ala)	0.044			α-*H*(Phg)	0.038
		Ar*H*	0.010			*CH*$_3$(Ts)	0.009			Ar*H*	0.059
		CO*NH*Ar[b]	0.026			Ar*H*	0.052			Ar*H*	0.061
	CSA **3**	*CH*$_3$(Ala)	0.017			CO*NH*(Phg)	0.103			CO*NH*Ph	0.080
		CH$_3$O	0.008			CO*NH*Ph	0.095		CSA **9**	Ph*CH*$_2$	0.017
		CO*NH*(Ala)	0.020		CSA **9**	α-*H*(Ala)	0.057			α-*H*(Phe)	0.048
		Ar*H*	0.015			α-*H*(Phg)	0.074			Ar*H*	0.049
	CSA **4**	*CH*$_3$(Ala)	0.010			Ar*H*	0.055	(±)-G**25**	CSA **1**	α-*H*(Phg)	0.006
		CH$_3$O	0.015	(±)-G**21**	CSA **1**	*CH*$_3$(Ala)	0.011		CSA **3**	α-*H*(Phg)	0.012
		Ts*NH*	0.035			O*CH*$_3$	0.004		CSA **4**	α-*H*(Phg)	0.007
		CO*NH*(Ala)	0.081		CSA **2**	Ts*NH*	0.022		CSA **5**	Ar*H*	0.049
		Ar*H*	0.029		CSA **3**	α-*H*(Phg)	0.010		CSA **6**	α-*H*(Phg)	0.012
		CO*NH*Ar[b]	0.040			Ts*NH*	0.018		CSA **7**	*CH*$_3$(Ts)	0.011
	CSA **5**	*CH*$_3$(Ala)	0.007			Ar*H*	0.008			α-*H*(Pro)	0.044
		CH$_3$(Ts)	0.007			CO*NH*(Phg)	0.020			α-*H*(Phg)	0.047
		CH$_3$O	0.010			CO*NH*Ar[b]	0.015			CO*NH*Ph	0.083

Guest	CSA	Proton	ΔΔδ	Guest	CSA	Proton	ΔΔδ	Guest	CSA	Proton	ΔΔδ
		CO*NH*(Ala)	0.068		CSA **4**	CH_3(Ala)	0.012		CSA **8**	α-*H*(Phg)	0.009
		CO*NH*Ar[b]	0.031			OCH_3	0.013			Ar*H*	0.019
	CSA **6**	CH_3(Ala)	0.004			α-*H*(Phg)	0.006			CO*NH*(Phg)	0.018
		CO*NH*(Ala)	0.020			Ts*NH*	0.085			CO*NH*Ph	0.013
		Ar*H*	0.004			Ar*H*	0.023		CSA **9**	α-*H*(Phg)	0.123
		CO*NH*Ar[b]	0.023			CO*NH*(Phg)	0.059			Ar*H*	0.057
	CSA **7**	CH_3(Ala)	0.079		CSA **5**	OCH_3	0.004			CO*NH*(Phg)	0.031
		CH_3(Ts)	0.048			α-*H*(Phg)	0.007	(±)-G**26**	CSA **3**	α-*H*(Phg)	0.010
		CH_3O	0.033			Ar*H*	0.010			CO*NH*(Phg)	0.007
		Ar*H*	0.047		CSA **6**	Ar*H*	0.011		CSA **6**	α-*H*(Phg)	0.013
		CO*NH*Ar[b]	0.183		CSA **7**	CH_3(Ts)	0.030		CSA **7**	CH_3(Ts)	0.018
	CSA **8**	CH_3(Ts)	0.022			OCH_3	0.046			*CH*(Pro)	0.085
		CH_3O	0.018			Ar*H*	0.037			OCH_3	0.031
		α-*H*(Ala)	0.070			Ar*H*	0.030			α-*H*(Pro)	0.073
		Ts*NH*	0.235		CSA **8**	CH_3(Ala)	0.038			Ar*H*	0.020
		Ar*H*	0.057			OCH_3	0.029			CO*NH*Ar[b]	0.138
		Ar*H*	0.056		CSA **9**	OCH_3	0.029		CSA **8**	OCH_3	0.016
		Ar*H*	0.014			α-*H*(Phg)	0.082			α-*H*(Phg)	0.019
	CSA **9**	CH_3(Ala)	0.073			Ar*H*	0.071			Ar*H*	0.019
		CH_3O	0.030			CO*NH*Ar[b]	0.061			Ar*H*	0.020
		Ts*NH*	0.097	(±)-G**22**	CSA **1**	CO*NH*(Phe)	0.089		CSA **9**	OCH_3	0.022
		Ar*H*	0.067			CO*NH*Ph	0.050			α-*H*(Pro)	0.040
		Ar*H*	0.047		CSA **2**	CO*NH*Ph	0.045			α-*H*(Phg)	0.125
(±)-G**18**	CSA **3**	Ts*NH*	0.021		CSA **3**	CH_3(Ala)	0.005			Ar*H*	0.051
	CSA **4**	CH_3(Ts)	0.006			Ts*NH*	0.018	(±)-G**27**	CSA **1**	CO*NH*Ph	0.016
		α-*H*(Phg)	0.031			CO*NH*(Phe)	0.055		CSA **2**	CO*NH*Ph	0.012
		Ts*NH*	0.127			CO*NH*Ph	0.035		CSA **3**	α-*H*(Phe)	0.008
	CSA **5**	Ts*NH*	0.049		CSA **4**	Ts*NH*	0.033			CO*NH*Ph	0.028
	CSA **7**	CH_3(Val)	0.016			CO*NH*Ph	0.083		CSA **4**	PhCH_2	0.005

Guest	CSA	Proton	$\Delta\Delta\delta$	Guest	CSA	Proton	$\Delta\Delta\delta$	Guest	CSA	Proton	$\Delta\Delta\delta$
		CH_3(Val)	0.047		CSA **5**	CH_3(Ts)	0.015		CSA **5**	CO*NH*Ph	0.017
		CH_3(Ts)	0.030			CO*NH*(Phe)	0.110		CSA **6**	CO*NH*Ph	0.032
		Ts*NH*	0.089			Ar*H*	0.019		CSA **7**	CH_3(Ts)	0.006
		Ar*H*	0.045		CSA **6**	CO*NH*(Phe)	0.066			*CH*(Pro)	0.059
		Ar*H*	0.029		CSA **7**	CH_3(Ala)	0.023			α-*H*(Pro)	0.057
	CSA **8**	CH_3(Ts)	0.025			Ar*H*	0.020			Ar*H*	0.019
		α-*H*(Phg)	0.037		CSA **8**	CH_3(Ts)	0.025		CSA **8**	Ar*H*	0.019
		Ar*H*	0.057			Ar*H*	0.018		CSA **9**	PhCH_2	0.018
		CO*NH*Ph	0.045		CSA **9**	CH_3(Ts)	0.023			α-*H*(Pro)	0.061
	CSA **9**	CH_3(Ts)	0.009			α-*H*(Phe)	0.072			Ar*H*	0.033
		Ts*NH*	0.086			Ts*NH*	0.140				
		Ar*H*	0.053	(±)-G**23**[c]	CSA **1**	CH_3O	0.005				

[a] $\Delta\Delta\delta = |\Delta\delta(S,R)\text{-G}\mathbf{X} - \Delta\delta(R,S)\text{-G}\mathbf{X}|$, $\Delta\delta(S,R)\text{-G}\mathbf{X} = \delta(S,R)\text{-G}\mathbf{X} - \delta_{free}$ $\Delta\delta(R,S)\text{-G}\mathbf{X} = \delta(R,S)\text{-G}\mathbf{X} - \delta_{free}$, (**X** = **16**–**27**), [Guest] = 5 mM, H:G = 1:1;

[b] Ar = 4-MeOC_6H_4;

[c] [Guest] = 4 mM;

[d] [Guest] = 2.5 mM;.

Table 4.

Association constants (K_a, M^{-1}) and ΔG^o (KJ mol^{-1}) of (*S*,*R*)-G**16** and (*R*,S)-G**16** with CSA **7**.[a]

Host	Guest	K_a	$-\Delta G^\circ$
CSA **7**	(*S*,*R*)-G**16**	$(5.55 \pm 5.20) \times 10^3$	18.7 ± 4.3
CSA **7**	(*R*,S)-G**16**	$(5.98 \pm 5.56) \times 10^3$	19.1 ± 4.1

[a] K_a values were calculated by the nonlinear curve-fitting method.

Table 5.

Calculated and observed chemical shift values (δ, ppm) and nonequivalent chemical shift values ($\Delta\delta$, ppm) for the *NH* (CO*NH*Ph) proton of the (*S*,*R*)-G**16** and (*R*,*S*)-G**16** in the presence of CSA **7**.

	$\delta_{(S,R)\text{-G16}}$	$\delta_{(R,S)\text{-G16}}$	$\Delta\delta$
Obsd values	8.540	8.355	0.185
Calcd vaues	8.633	8.516	0.117